Quaternary Research 84 (2015) 255–261

Contents lists available at ScienceDirect

Quaternary Research

journal homepage: www.elsevier.com/locate/yqres

Peatland evolution and associated environmental changes in central China over the past 40,000 years

Yuxin He [a,b,*], Cheng Zhao [b,c,**], Zhuo Zheng [d], Zhonghui Liu [b], Ning Wang [b,e], Jie Li [d], Rachid Cheddadi [f]

[a] Department of Earth Sciences, Zhejiang University, Hangzhou 310027, China
[b] Department of Earth Sciences, The University of Hong Kong, Hong Kong, China
[c] State Key Laboratory of Lake Science and Environment, Nanjing Institute of Geography and Limnology, Chinese Academy of Sciences, Nanjing 210008, China
[d] Department of Earth Sciences, Sun Yat-sen University, Guangzhou 510275, China
[e] Guangzhou Institute of Geochemistry, Chinese Academy of Sciences, Guangzhou 510640, China
[f] Institut des Sciences de l'Evolution de Montpellier, CNRS-UM2, Montpellier 34095, France

ARTICLE INFO

Article history:
Received 14 November 2014
Available online 26 June 2015

Keywords:
Central China
n-Alkanes
Hopanes
Dajiuhu peatland
Marine Isotope Stages 1–3

ABSTRACT

Central China has experienced stronger summer monsoon during warm periods such as Marine Isotope Stages (MIS) 1 and 3, and weaker summer monsoon during cool periods such as MIS 2. The evolution history of Dajiuhu subalpine peatland in central China can help investigate how the expansion and shrinkage of peatland were associated with monsoonal strength over the last glacial–interglacial cycle. Here we apply bulk organic carbon and molecular biomarkers (hopane and *n*-alkane) to reconstruct the evolution history for the Dajiuhu peatland over the past 40,000 yr. The results indicate fluctuations between lacustrine and peat-like deposition during MIS 3, steady lacustrine deposition during MIS 2, and peatland initiation and expansion during MIS 1 in the Dajiuhu peatland. Therefore, at the glacial–interglacial scale, warmer summer and cooler winter conditions in interglacial periods are crucial to trigger peat deposition, whereas reduced evaporation in glacial period instead of decreased monsoonal-driven precipitation would have played a predominant role in the regional effective moisture balance. However, within the Holocene (MIS 1), monsoonal precipitation changes appear to be the main controller on millennial-scale variations of water-table level of the Dajiuhu peatland.

Introduction

The Asian summer monsoon is an important atmospheric circulation system maintaining the living environment on the Asian continent. Climatic changes throughout the late Quaternary in the East Asia are characterized by alternations of the Asian summer monsoon strength (An, 2000). High-quality $\delta^{18}O$ records from cave stalagmites suggest that central China has experienced stronger summer monsoon during warm periods such as Marine Isotope Stages (MIS) 1 and 3, and weaker summer monsoon during cool periods such as MIS 2 (Wang et al., 2001, 2008). However, knowledge of climatic variations and their relation with ecosystem evolution in central China over the last interglacial–glacial cycle (MIS 1–3) remains incomplete, owing to limited high-quality paleoclimatic records available other than speleothem $\delta^{18}O$ records (Wang et al., 2001, 2008; Herzschuh, 2006).

Peatland serves as a good archive for paleoclimatic reconstruction, since expansion and shrinkage of peatland respond sensitively to climatic changes. Understanding how peatland development was associated with past climatic conditions would provide useful insights into projecting future environmental changes. Most previous peatland studies have focused on two major zones, high latitude regions (50°–70°N) and tropical regions (20°S–10°N; Zhao et al., 2014). Abundant peatlands in northern and tropical China, such as Hani (Zhou et al., 2010), Hongyuan (Zheng et al., 2007) and Dingnan bogs (Zhou et al., 2005; see locations in Fig. 1A) could offer important information on peatland histories in the mid-latitude region of the Northern Hemisphere (20°–50°N), connecting the two major peatland regions. The Dajiuhu peatland is a well-preserved subalpine peatland in the western Shennongjia Mountains in central China (~30°N). Thick and continuous peat deposits allow for the reconstruction of past environment and climate changes (Zhu et al., 2010). Because the nearby Sanbao Cave contains high-quality monsoonal records over the last glacial–interglacial cycle (Fig. 1A, Wang et al., 2008), records from the Dajiuhu peatland would provide a good opportunity to disentangle the relation between the peatland ecosystem evolution and monsoonal strength in this region.

Recent developments in organic geochemistry have introduced molecular biomarkers to paleoclimatic reconstruction (Eglinton and

* Correspondence to: Y. He, Department of Earth Sciences, Zhejiang University, Hangzhou 310027, China.
** Correspondence to: C. Zhao, State Key Laboratory of Lake Science and Environment, Nanjing Institute of Geography and Limnology, Chinese Academy of Sciences, Nanjing 210008, China.
E-mail addresses: yxhe@zju.edu.cn (Y. He), czhao@niglas.ac.cn (C. Zhao).

http://dx.doi.org/10.1016/j.yqres.2015.06.004
0033-5894/

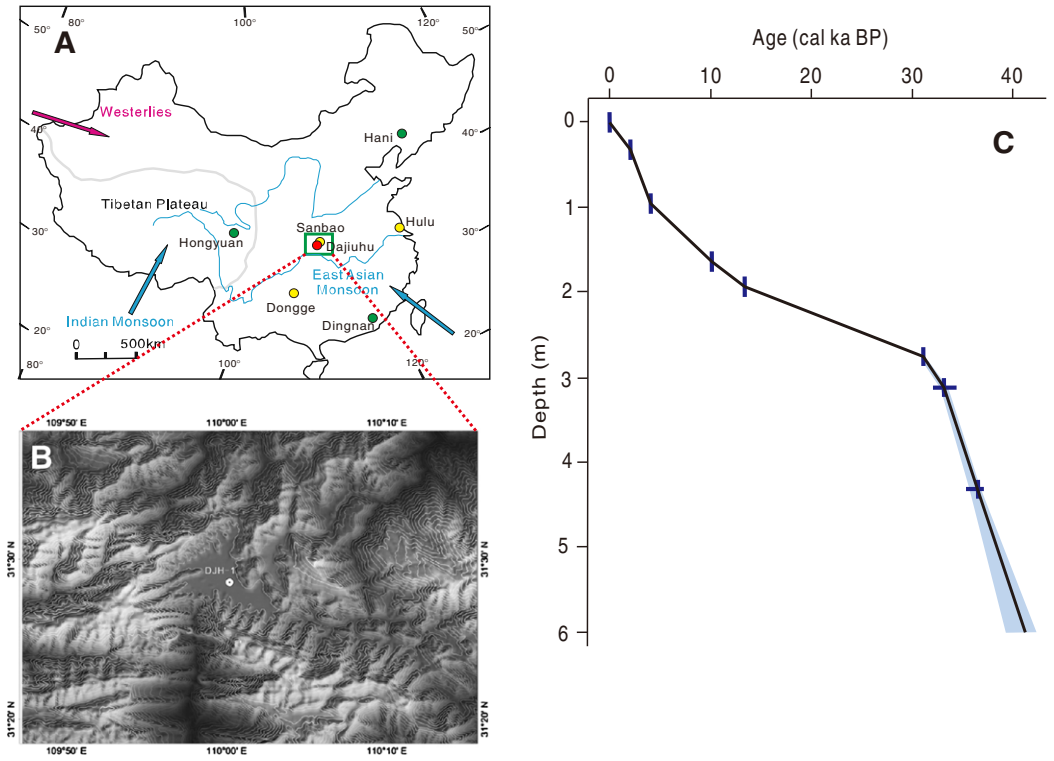

Figure 1. (A) Overview map showing location of the Dajiuhu (red dot), Hongyuan, Dingnan and Hani peat bog (green dots) and Dongge, Sanbao and Hulu Caves (yellow dots). (B) Coring site of core DJH-1. (C) Age profile for core DJH-1 based on seven AMS ^{14}C dates (Li et al., 2013).

Eglinton, 2008; Castañeda and Schouten, 2011). Many types of biomarkers have been utilized to infer climatic changes in the Dajiuhu region, including branched fatty alcohols (Huang et al., 2013a), hopanoids (Xie et al., 2013) and aromatic triterpenes (Huang et al., 2013b). However, none of these studies involve *n*-alkanes, a traditional biomarker for both lacustrine (e.g., He et al., 2014) and peatland studies (e.g., Bingham et al., 2010; Zhou et al., 2010). A set of *n*-alkane indices, including the average chain length (ACL, Poynter and Eglinton, 1990), the odd-over-even carbon preference index (CPI, Marzi et al., 1993) and the proportion of aquatic macrophytes (P_{aq}, Ficken et al., 2000) can be good supplementary indicators on vegetation composition variation and peatland evolution. On the other hand, previous studies (Huang et al., 2013a, 2013b; Xie et al., 2013) have only focused on climatic conditions over the past 13,000 yr when the peatland was fully formed, barely allowing for reconstructions at glacial–interglacial timescales. How the Dajiuhu peatland itself evolved and how its evolution was associated with climatic conditions over the last glacial–interglacial cycle largely remain elusive. In view of that, here we reconstruct bulk organic carbon and molecular biomarker (hopane and *n*-alkane) records obtained from a 6-m core taken from the Dajiuhu peatland at central China. Together with previously presented lithological, gray scale and pollen data from the same core (Li et al., 2013), we investigate the history of peatland evolution and regional environmental changes over the past 40,000 yr. Our objective is to infer the controlling mechanisms for the peatland formation over glacial–interglacial cycles and during the current interglacial period (i.e. the Holocene).

Materials and methods

The Dajiuhu peatland (110°00′E, 31°29′N, 1751 m above sea level) is located at the western Shennongjia Mountains, which belong to the eastern extension of the Daba Mountain Ranges of the upper-middle reaches of the Yangtze River, central China (Figs. 1A, 1B). At present, this area is marked by short warm–wet summers and long cold–dry winters due to the influence of the Asian monsoons. Modern mean annual rainfall in this region is ~1550 mm, with 40–50% falling in the summer, and potential evaporation varies from 500 to 800 mm (Li et al., 2013).

A 6-m core (DJH-1) was collected from the Dajiuhu peatland using a Russian-type peat corer (Fig. 1B). The age profile of core DJH-1 has been described previously in Li et al. (2013). Chronologies were established through seven accelerator mass spectrometry (AMS)-^{14}C dates on the bulk organic matter (Table 1). Dating samples were pretreated at Guangzhou Institute of Geochemistry, CAS and analyzed in the AMS Lab at Beijing University. All dates were calibrated to calendar years with the CALIB 6.0.1 software (Stuiver and Reimer, 1993) using the IntCal09 database (Reimer et al., 2009). The age model for core DJH-1 was established using the Clam software package (Blaauw, 2010) including extrapolations to the top and bottom of the core. The total organic carbon (TOC) content was analyzed by the Euro EA3000 elemental analyzer. A low resolution TOC record from core DJH-1 has been reported in Li et al. (2013), and here we report an updated higher resolution one.

A total of 187 peat/sediment samples with the thickness of 1 cm from core DJH-1 were selected for lipid analysis. Total lipids were ultrasonically extracted from freeze-dried sediments with organic solvents

Table 1
AMS-^{14}C dates for the core DJH-1 chronology.

Laboratory ID	Depth (cm)	Materials	^{14}C age (^{14}C yr BP)	Error (yr)	Calendar age (cal yr BP)	Error (yr)
XA6289	33	Peat	2025	24	1982	62
GZ3136	95	Wood	3669	26	4003	82
XA6290	163	Peat	8894	40	10,039	151
GZ3137	193	Peat	11,533	39	13,375	107
XA6291	276	Sediment	26,640	105	31,069	168
GZ3138	312	Sediment	28,665	98	33,085	406
GZ3139	431	Wood	31,936	119	36,522	258

https://doi.org/10.1016/j.yqres.2015.06.004 Published online by Cambridge University Press

(dichloromethane: methanol = 9:1, *v*/*v*). After being hydrolyzed with 6% KOH in methanol solution, the neutral lipids were extracted with *n*-hexane. The neutral lipids containing *n*-alkanes and hopanes were then further cleaned using silica gel column chromatography. After identification by gas chromatography equipped with a mass spectrometry (GC-MS), *n*-alkanes ($m/z = 57$) and hopanes ($m/z = 191$, Fig. 2C) were quantitatively analyzed on the GC equipped with a flame ionized detector (FID, Figs. 2A, 2B). Quantification of *n*-alkane and hopane compounds was achieved by comparison of peak areas with *n*-C_{36} alkane external standard of known concentration.

The total *n*-alkane concentration was calculated by adding *n*-alkane components ranging from C_{21} to C_{33}, while the total hopane concentration was calculated by adding hopane components of C_{27}-17β(H)21β(H), C_{27}-17α(H)21β(H), C_{29}-17β(H)21α(H), C_{29}-17β(H)21β(H), C_{30}-17α(H)21β(H), C_{31}-17α(H)21β(H), C_{31}-17β(H)21α(H) and C_{31}-17β(H)21β(H).

The *n*-alkane ratio-based proxies were calculated as following:

$$ACL = (21 \times C_{21} + 23 \times C_{23} + 25 \times C_{25} + \ldots + 33 \times C_{33}) / (C_{21} + C_{23} + C_{25} + \ldots + C_{33})$$ (Poynter and Eglinton, 1990);

$$CPI = (C_{21} + C_{23} + C_{25} + \ldots + C_{33}) / (C_{22} + C_{24} + C_{26} + \ldots + C_{32}) \times (7/8)$$ (Marzi et al., 1993);

$$P_{aq} = (C_{23} + C_{25}) / (C_{23} + C_{25} + C_{29} + C_{31})$$ (Ficken et al., 2000);

where C_i is the concentration of *n*-alkane of i number carbon. Analytical uncertainty for quantification of individual organic compounds is within 5% and the uncertainty for the ratio-based proxies is even smaller.

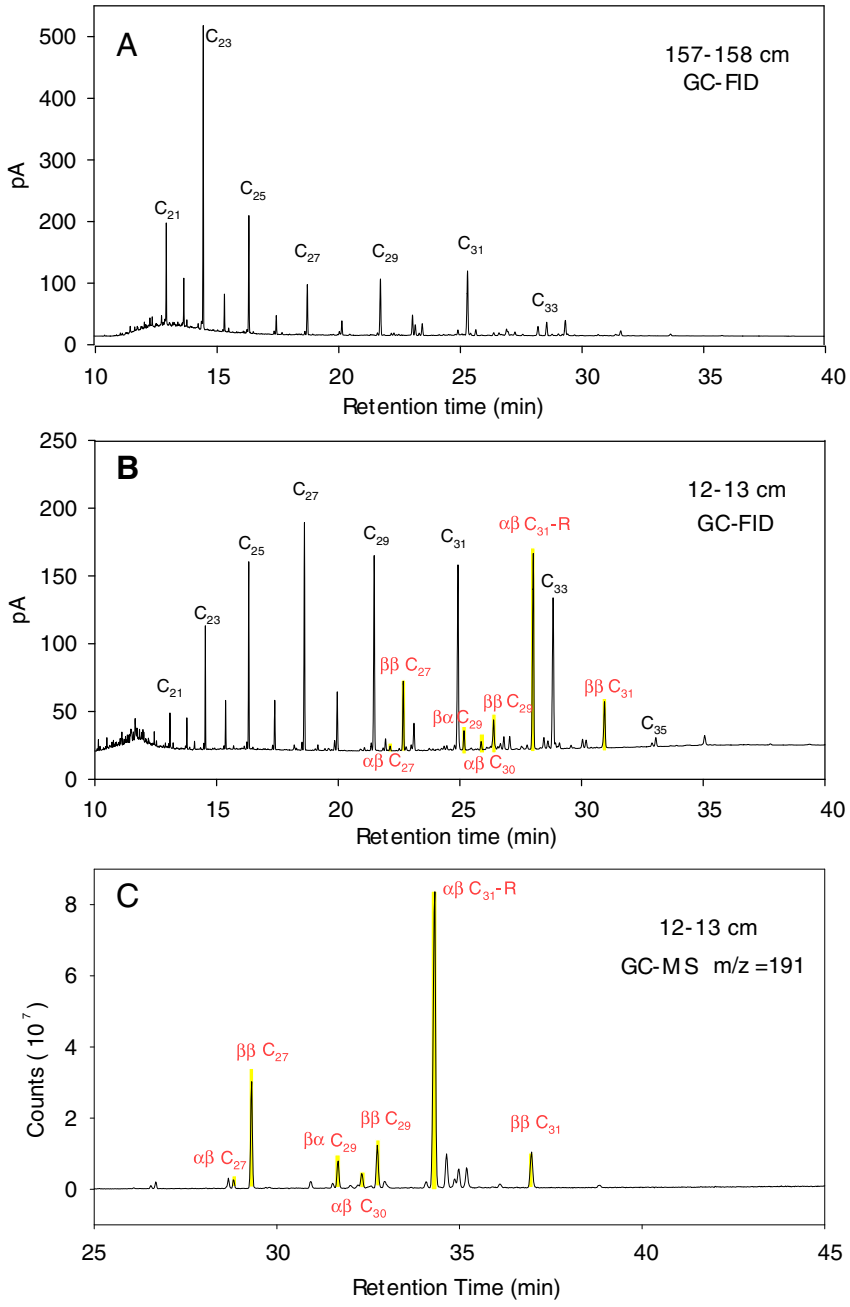

Figure 2. Representative GC-FID chromatograms of *n*-alkanes (black notations) and hopanes (red notations and yellow shadings) in samples at (A) 157–158 cm depth and (B) at 12–13 cm depth in core DJH-1. (C) GC-MS ion chromatogram ($m/z = 191$) of hopanes (red notations and yellow shadings) in the sample at 12-13 cm depth in core DJH-1.

https://doi.org/10.1016/j.yqres.2015.06.004 Published online by Cambridge University Press

Results

The upper part of core DJH-1 (0–2 m) is mainly composed of dark peat sediments, whereas the lower part (2–6 m) turns into gray clay and mud (see the lithological profile in Li et al., 2013). Since no coarse grain particles were observed in the lower part of this core, we suggest that sediments at that period were deposited in a lacustrine condition rather than in shallow-water or loess environments. Sediments at the depth of 2–2.7 m are mainly composed by gray clays with lighter color and those at the depth of 2.7–6 m are darker, suggesting a slightly higher bio-productivity at the 2.7–6 m section.

Based on the derived chronology (Fig. 1C; Li et al., 2013), core DJH-1 covers the past 40,000 yr. The sedimentation rate is ~0.2 mm/yr at 40–30 cal ka BP and 10–0 cal ka BP, whereas it is ~0.1 mm/yr at 30–10 cal ka BP, consistent with the previous study (Zhu et al., 2010). The concentrations of *n*-alkanes and hopanes in core DJH-1 varied substantially throughout the core, from 800 ng/g to 2×10^6 ng/g for *n*-alkanes and from 10 ng/g to 10^5 ng/g for hopanes, respectively (Fig. 3). The *n*-alkane and hopane concentrations share a similar variation pattern. During 40–25 cal ka BP, the *n*-alkane and hopane concentrations were generally low, except for short periods near 31, 33, 35, 37, and 38.5 cal ka BP with low to moderate *n*-alkane and hopane occurrences. During 25–14 cal ka BP, the *n*-alkane and hopane occurrences stayed at extremely low values. Starting at ~14 cal ka BP, the *n*-alkane and hopane occurrences increased to reach the highest value at 2 cal ka BP. After 2 cal ka BP, the *n*-alkane and hopane occurrences dropped to low values similar to those during 40–14 cal ka BP. The TOC record shares a similar trend with *n*-alkane and hopane concentrations. The TOC values range from almost 0 to 47%. During 40–14 cal ka BP, the TOC content also remained in low values except for short periods at near 31, 33, 35, 37, and 38.5 cal ka BP, consistent with the *n*-alkane and hopane occurrences. The TOC content started to increase at 14 cal ka BP, but it was not until 9 cal ka BP when the TOC content increased abruptly. After 2 cal ka BP, the TOC content started to drop to 10–20%.

In order to avoid over-interpretation of *n*-alkane ratio-based proxies, we only present these records over the past 14,000 yr (Fig. 4), when the occurrence of *n*-alkanes is high enough. CPI values (Fig. 4E) range from 1.6 to 6.8 over the last 14,000 yr. During 14–10 cal ka BP, CPI stayed at ~4. Then CPI increased abruptly at 10 cal ka BP and reached the maximum value of 6.8 at 5 cal ka BP. After 5 cal ka BP, CPI gradually declined to 3 at 1–0 cal ka BP.

ACL values range from 25.8 to 29.4. ACL (Fig. 4D) stayed around 28 during 14–12 cal ka BP. At 12 cal ka BP, ACL decreased abruptly and reached the minimum value of 25.8 at around 10 cal ka BP. Since then ACL increased to ~28.9 at 6 cal ka BP. ACL increased again at 4 cal ka BP and reached ~27 at 3 cal ka BP and then dropped back to ~29 at 2 cal ka BP. Over the last 2 cal ka BP, ACL remained at high values (28.5–29.3).

P_{aq} shows a consistently opposite pattern from ACL (Fig. 4D). P_{aq} values range from 0.17 to 0.64, with the maximum value at 10 cal ka BP and the minimum at 2 cal ka BP. The P_{aq} record also shows two periods of high values (~0.6) centered around 12 cal ka BP and 4 cal ka BP, corresponding to the periods of low ACL values. For other periods, P_{aq} values are relatively small, around 0.3–0.4.

Discussion

n-Alkanes and hopanes for peatland evolution indication

Two distinctive *n*-alkane distribution patterns are observed through core DJH-1, one dominated by both mid-chain (C_{23}–C_{25}) and long chain (C_{29}–C_{31}) *n*-alkanes and the other dominated only by long chain *n*-alkanes with a distinct odd-over-even carbon predominance (Fig. 2). Therefore, ACL, CPI and P_{aq} are indicative of oscillations between these two *n*-alkane types. It has been suggested that the C_{23}–C_{25} *n*-alkane homologues are mainly from submerged and floating macrophytes in both lakes and peatlands (Baas et al., 2000; Ficken et al., 2000; Pancost et al., 2002; Mead et al., 2005; Nichols et al., 2009; Bingham et al., 2010). In contrast, *n*-alkanes from the typical vascular plants are dominated by the C_{29}–C_{31} components with a distinct odd-over-even carbon predominance (Ficken et al., 2000; Bi et al., 2005; Sachse et al., 2006). An increase of submerged macrophytes in combination with the recession of vascular plants could lead to lower ACL, lower CPI and higher P_{aq} values. This notion is supported by the synchronous high P_{aq} values and *Sphagnum* pollen occurrences at 12–10 cal ka BP (Li et al., 2013). Furthermore, *n*-alkane concentrations can be another good supplementary proxy for peatland productivities, since the peatland environment would conduct massive *n*-alkane input.

Produced by microbacteria favoring aerobic conditions, hopanes and hopanoids are capable of tracking aerobic bacterial biomass resulting from hydrological changes in the Dajiuhu region (Xie et al., 2013). Moderate or high hopane occurrence is indicative of peatland initiation from a lacustrine environment when its water-table level is lower (Jaatinen et al., 2007). On the other hand, in a peatland environment, the redox condition is mainly controlled by the water-table level above the peatland (Jaatinen et al., 2007). Accordingly, hopane occurrence can also be a good indicator of the water-table level above the peatland. Such a notion is supported by the surface sample data from the Dajiuhu region, indicating increasing hopane and hopanoid contents with lowering water-table level (Xie et al., 2013). For the purpose of minimizing

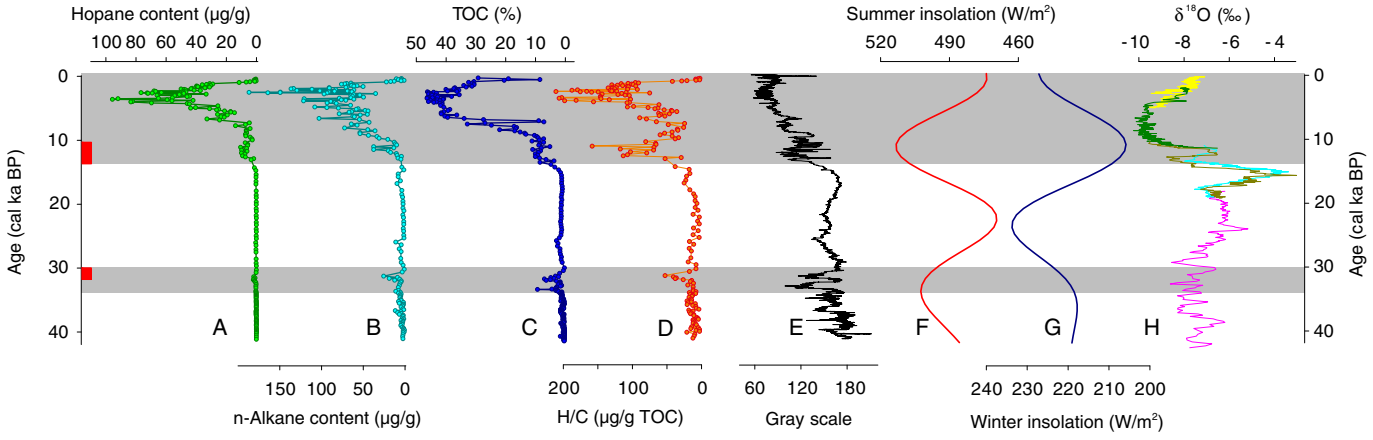

Figure 3. Comparison of (A) hopane concentration, (B) *n*-alkane concentration, (C) TOC, (D) H/C ratio and (E) gray scale index (Li et al., 2013) records from core DJH-1 over the last 40,000 yr with (F) summer insolation at 30°N (Berger and Loutre, 1991), (G) winter insolation at 30°N (Berger and Loutre, 1991) and (H) combined $\delta^{18}O$ records from Sanbao Cave (Wang et al., 2008) and Hulu Cave (Wang et al., 2001; colors indicating different records). Red bars indicate periods of appearance of *Sphagnum* pollen from core DJH-1 (Li et al., 2013). Gray shadings indicate peat and peat-like deposition phases.

https://doi.org/10.1016/j.yqres.2015.06.004 Published online by Cambridge University Press

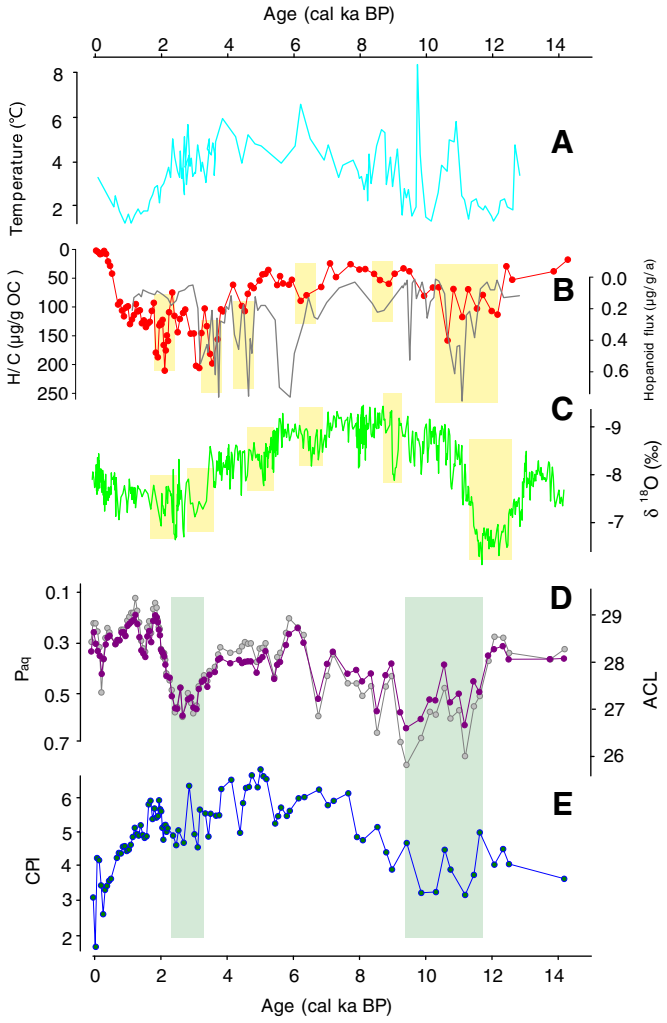

Figure 4. Comparison of (B) H/C ratio from core DJH-1 (red) and hopanoid flux record from core DJH-CUG from Dajiuhu peatland (gray, Xie et al., 2013) with (A) reconstructed temperature record from core DJH-CUG (cyan, Huang et al., 2013a) and (C) $\delta^{18}O$ record from Dongge Cave (green, Dykoski et al., 2005) over the past 14,000 yr. For (B) and (C), yellow bars indicate the concurring water-table level lowering and weaken monsoon intensity events. (D) *n*-Alkane based ACL (gray) and P_{aq} (dark pink) records from core DJH-1 over the past 14,000 yr. (E) *n*-Alkane based CPI record from core DJH-1 over the past 14,000 yr. Green shadings in (D) and (E) indicate two periods with low ACL, low CPI and high P_{aq} values.

the influence of organic deposition flux on hopane occurrence, the hopane record from core DJH-1 was further normalized with the TOC content (referred as H/C proxy, Fig. 3D, some interpolations were created due to different resolutions between the two records). A similar trend between hopane contents and the H/C record (Figs. 3A, 3D) suggests that hopane concentrations are independent from total organic deposition and capable of indicating water-table level variations.

Peatland evolution history over the past 40,000 yr

Based on our records from core DJH-1, the environmental change in the Dajiuhu region over the past 40,000 yr can be divided into the following three stages (Fig. 3):

Stage I: 40–30 cal ka BP (MIS 3)
For most time at this stage, our records of *n*-alkane occurrences, hopane occurrences, the TOC content and the gray scale index all stayed in low values, suggesting that the Dajiuhu region was in a lacustrine condition with relatively low biomass input. However, moderate values of these indices superimposing on the low biomass background at near 31, 33, 35, 37 and 38.5 cal ka BP imply that the Dajiuhu region occasionally experienced peat-like conditions, roughly occurring at every ~2000 yr. The water level in this peat-like environment was between that of peatland and lake environments. The appearance of *Sphagnum* pollen (Li et al., 2013) at 31–30 cal ka BP, coinciding with relatively high hopane and *n*-alkane concentrations, also supports this peat-like condition. According to the plot of ACL vs. *n*-alkane concentration (Fig. 5), the negative relation during 40–30 cal ka BP implies that the main source of *n*-alkane in this stage is macrophytes instead of vascular plants and the Dajiuhu region varied between lake and swamp (or *Sphagnum*-dominated peat). Otherwise, if a well-developed peatland occurred at this period, terrestrial plants should dominate in this region and a positive relation of ACL vs. *n*-alkane occurrence would be observed. Therefore, we believe that the Dajiuhu region experienced the peat-like formation with a water-table level favoring growth of macrophytes at this stage, which did not last long enough for the development of terrestrial-dominated peatland.

Stage II: 30–14 cal ka BP (MIS 2)
This stage is known as reduced insolation and weakened summer monsoons (Cosford et al., 2010). *n*-Alkane concentrations, hopane concentrations and the TOC content are close to 0 except for a short period at 26–25 cal ka BP, indicating very low biomass input at the stage. The extremely low TOC content, together with lack of *Sphagnum* pollen would essentially rule out a shallow water environment, leaving an eolian deposit or a deep-water lacustrine environment as two plausible interpretations. We suggest that the most likely interpretation of this part of the sequence is of a lacustrine environment, based on the lithological properties (grain size and color) in this section (Li et al., 2013). The gray scale index record also remained at low value with no obvious variations (Fig. 3E), consistent with the light gray clay observed in this section. Thus the Dajiuhu region most likely remained at a stable lacustrine condition at this stage with the lowest depositional rate (~0.1 mm/yr) through the core, probably due to relatively cool climates (Wang et al., 2001, 2008; Cosford et al., 2010).

Stage III: 14–0 cal ka BP (MIS 1 or Holocene)
Rapid initiation and expansion of the peatland occurred in the Dajiuhu region after MIS 2, probably triggered by the onset of deglacial warming at the late Pleistocene-Holocene transition (~13 cal ka BP). The relation of ACL vs. *n*-alkane concentrations

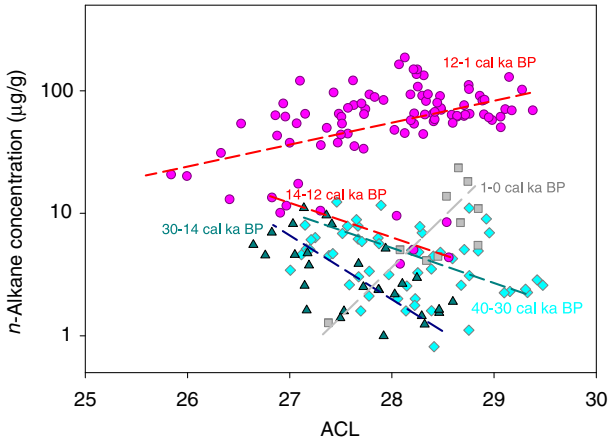

Figure 5. Comparison of *n*-alkane concentrations and ACL values across different periods: 40–30 cal ka BP (cyan dots with dark cyan regression line), 30–14 cal ka BP (dark cyan dots with blue regression line), 14–1 cal ka BP (purple dots with red regression lines) and 1–0 cal ka BP (gray dots with gray regression line).

https://doi.org/10.1016/j.yqres.2015.06.004 Published online by Cambridge University Press

shifted from negative (14–12 cal ka BP) to positive (12–1 cal ka BP) at the transition (Fig. 5), suggesting that the high *n*-alkane concentration at 12–1 cal ka BP is indicative of the development of terrestrial-dominated peat over *Sphagnum*-dominated peat. The increase of *n*-alkane concentrations, hopane concentrations and the TOC content confirms the high biomass production thus the peat bog development in the region (Fig. 3). During the late Holocene (3–0 cal ka BP), a decrease of the peatland productivity and a recession of arboreal plants are observed, probably related to cooler climates in the region (Huang et al., 2013a).

In summary, our records of *n*-alkane concentrations, hopane concentrations and the TOC content indicate occasional peat-like depositions during MIS 3, steady lacustrine deposition during MIS 2, and peat initiation and intensive expansion during MIS 1 in the Dajiuhu region. According to $\delta^{18}O$ records from the nearby Sanbao Cave (Wang et al., 2008) and Hulu Cave (Wang et al., 2001), climates in central China were wet at MIS 3, dry at MIS 2 and much wetter at MIS 1, which is broadly consistent with the Dajiuhu peatland evolution history, but in an opposite sense. Thus monsoon-induced precipitation could not be the main factor controlling the lake–peat transition in the subtropical region over the last glacial–interglacial cycle. We thus suggest that higher insolation-induced temperature instead of monsoon-driven precipitation is more crucial in triggering the peatland initiation at orbital timescales over the past 40,000 yr. Peat and peat-like depositions might be attributed to both high summer insolation leading to increased productivity and low winter insolation leading to reduced decomposition (Fig. 3, Berger and Loutre, 1991; Jones and Yu, 2010). Also, during MIS 2 when the Asian Summer Monsoon was much weaker, the steady lacustrine condition, however, remained in the Dajiuhu region. Therefore, reduced evaportranspiration in lower temperatures must be the key to maintain the lacustrine environment.

Climate changes over the past 14,000 yr

After the Dajiuhu peatland formed at ~14 cal ka BP, high contents of hopanes and *n*-alkanes provide an opportunity to reveal detailed environmental changes in the Dajiuhu region. Our data, together with previous records (e.g. Huang et al., 2013a, 2013b; Xie et al., 2013), would help infer the history of peatland evolution and potential controlling factors, as well as the application of hopane and *n*-alkane proxies.

Considering the chronological uncertainty and different magnitudes, the H/C ratio roughly shares a similar pattern with the hopanoid flux record from another sediment core of the Dajiuhu peatland (Fig. 4B; Xie et al., 2013). According to both H/C ratio and hopanoid flux records (Xie et al., 2013), the water-table level stayed relatively high during 14–12 cal ka BP, prior to the Dajiuhu peatland initiation. Then the water-table level dropped at 12 cal ka BP but recovered quickly at 11 cal ka BP. During 10–5 cal ka BP, the water-table level in the Dajiuhu peatland remained at a relatively high level, corresponding to the Holocene Climate Optimum. After then, the water-table level gradually lowered from 5 cal ka BP to 3 cal ka BP. Over the last 2000 yr, the water-table gradually increased to a level similar to that at 10–5 cal ka BP. According to the temperature record from the Dajiuhu peatland (Fig. 4A; Huang et al., 2013a), the climate was warmer during 8–3 cal ka BP and colder at 3–0 cal ka BP and 13–9 cal ka BP in this region, indicating a good correlation between water-table level and temperature variations from the Dajiuhu peatland during the Holocene, with increased temperature corresponding to higher water-table level. It thus rules out the significant effect of temperature-induced evaportranspiration on water-table level variation.

Over the past 14 cal ka BP, lower water-table level of the Dajiuhu peatland corresponded to lower Asian Summer Monsoon intensity as inferred from the $\delta^{18}O$ record from Dongge Cave (Fig. 4C, Dykoski et al., 2005). Both the Dajiuhu peatland water-table level and the Asian Summer Monsoon intensity show an abrupt increase starting at ~12 cal ka BP. The relatively high water-table level during 10–5 cal ka BP is broadly consistent with strong monsoon intensity. The water-table level lowering during 5–3 cal ka BP is largely synchronous with the gradually declining trend of the summer monsoon intensity. The gradually increased water-table level indeed resembles the increase in the Asian summer monsoon strength during the late Holocene (Zhao et al., 2013). Further, the millennial-scale water-table level lowering events centered at about 11.0, 8.2, 6.0, 4.1, 3.7, and 2.1 cal ka BP also appear to correspond to periods of Asian Summer Monsoon weakening (Fig. 4C, Dykoski et al., 2005). Therefore, over the past 14,000 yr, the monsoonal precipitation might be the main control on millennial-scale water-table level variations in the Dajiuhu region.

The *n*-alkane-based proxies ACL, CPI and P_{aq} can also help decipher the history of climate change, vegetation composition and peatland evolution over the past 14,000 yr (Figs. 4D, 4E). Interestingly, the *n*-alkane proxy records show both similarities and differences with the H/C ratio and the hopanoid flux data (Fig. 4B, Xie et al., 2013). The main reason might be that *n*-alkanes were also influenced by factors other than the water-table level, such as vegetation compositions, temperatures and moisture availabilities. In this sense, sole *n*-alkane proxy record could sometimes be explained in different directions and requires careful examination together with other proxies (He et al., 2014).

During 12–10 and 3–2 cal ka BP, low CPI, low ACL and high P_{aq} values are observed (Figs. 4D, 4E), indicating higher submerged macrophyte biomass input. At 12–10 cal ka BP, abundant *Sphagnum* pollen is observed, supporting the idea of higher submerged macrophyte biomass input (Li et al., 2013). At 3–2 cal ka BP, although the TOC and the *n*-alkane concentration remain in steady values and no *Sphagnum* pollen is found at the section (Li et al., 2013), an enrichment of bulk organic carbon isotope still implies an increased input of submerged macrophyte biomass (Li et al., 2013). According to the H/C ratio and the hopanoid flux, the water-table level above the Dajiuhu peatland was relatively low during 12–10 cal ka BP and 3–2 cal ka BP. Relatively low water-table level caused by low precipitation would favor the growth of submerged macrophytes. Interestingly, at ~2 cal ka BP and 4–3 cal ka BP when the water-table level was lowest, relatively high CPI, high ACL and low P_{aq} values are observed (Fig. 4), suggesting that the growth of submerged macrophytes would be confined in certain water depth, neither too deep nor too shallow.

During 9–4 cal ka BP, high CPI, high ACL and low P_{aq} suggest that *n*-alkanes were of the terrestrial plant source, synchronous with the appearance of the arboreal pollen, probably due to the expansion of hard-wood forests (Li et al., 2013). Such a forest expansion and the synchronously high water-table level might be caused by warm-wet climates at the mid-Holocene Optimum. Over the past 2000 yr, ACL/P_{aq} ratios remained in high/low values whereas CPI data decreased significantly to the minimum value (~1). According to the high water-table level suggested by the H/C ratio and the hopanoid flux (Xie et al., 2013), such *n*-alkane signals might be induced by some unknown aquatic vascular plants synthesizing *n*-alkanes of high ACL and low CPI values. But more possibly, the extremely low CPI values could be modified by greater microbial reworking of *n*-alkanes and/or oil contaminants with *n*-alkanes of low CPI values caused by increasing anthropogenic activities around the region (Xie et al., 2013).

Conclusion

This study provides biomarker evidence for the peatland evolution history in the Dajiuhu region at central China, over the past 40,000 yr. The records suggest occasional peat-like depositions during MIS 3, steady lacustrine deposition during MIS 2, and peat initiation and intensive peat expansion during MIS 1. The peat and peat-like conditions occurring during MIS 1 and 3 suggest that warmer summer and cooler winter conditions in interglacial periods instead of strong monsoon-driven precipitation are more crucial to trigger the Dajiuhu peatland initiation. The steady lacustrine environment during cooler MIS 2, as

https://doi.org/10.1016/j.yqres.2015.06.004 Published online by Cambridge University Press

compared to peat and peat-like conditions during warmer MIS 1 and 3, indicates that in the Dajiuhu region, temperature-induced evaporation might overprint monsoonal precipitation in modifying water-table level in cooler periods at orbital timescales. Further, our biomarker data together with the previous results suggest that the Dajiuhu peatland strongly responded to climate changes over the last 14,000 yr. Within the Holocene, monsoonal precipitation might be the main factor on millennial-scale water-table level changes.

Acknowledgment

This project was supported by the Hong Kong Research Grants Council (HKU 707612P), the National Natural Science Foundation of China (NSFC 41230101), the Fundamental Research Funds for the Central Universities (2015QNA3017), the Zhejiang Provincial Natural Science Foundation of China (LY15D030001) and the "Hundred Talents Program" of CAS to C. Zhao.

References

An, Z., 2000. The history and variability of the East Asian paleomonsoon climate. Quaternary Science Reviews 19, 171–187.

Baas, M., Pancost, R., van Geel, B., Damste, J.S.S., 2000. A comparative study of lipids in *Sphagnum* species. Organic Geochemistry 31, 535–541.

Berger, A., Loutre, M.F., 1991. Insolation values for the climate of the last 10 million years. Quaternary Science Reviews 10, 297–317.

Bi, X., Sheng, G., Liu, X., Li, C., Fu, J., 2005. Molecular and carbon and hydrogen isotopic composition of n-alkanes in plant leaf waxes. Organic Geochemistry 36, 1405–1417.

Bingham, E.M., McClymont, E.L., Väliranta, M., Mauquoy, D., Roberts, Z., Chambers, F.M., Pancost, R.D., Evershed, R.P., 2010. Conservative composition of *n*-alkane biomarkers in Sphagnum species: implications for palaeoclimate reconstruction in ombrotrophic peat bogs. Organic Geochemistry 41, 214–220.

Blaauw, M., 2010. Methods and code for 'classical' age-modelling of radiocarbon sequences. Quaternary Geochronology 5, 512–518.

Castañeda, I.S., Schouten, S., 2011. A review of molecular organic proxies for examining modern and ancient lacustrine environments. Quaternary Science Reviews 30, 2851–2891.

Cosford, J., Qing, H., Lin, Y., Eglington, B., Mattey, D., Chen, Y., Zhang, M., Cheng, H., 2010. The East Asian monsoon during MIS 2 expressed in a speleothem $\delta^{18}O$ record from Jintanwan Cave, Hunan, China. Quaternary Research 73, 541–549.

Dykoski, C.A., Edwards, R.L., Cheng, H., Yuan, D., Cai, Y., Zhang, M., Lin, Y., Qing, J., An, Z., Revenaugh, J., 2005. A high-resolution, absolute-dated Holocene and deglacial Asian monsoon record from Dongge Cave, China. Earth and Planetary Science Letters 233, 71–86.

Eglinton, T.I., Eglinton, G., 2008. Molecular proxies for paleoclimatology. Earth and Planetary Science Letters 275, 1–16.

Ficken, K.J., Li, B., Swain, D.L., Eglinton, G., 2000. An *n*-alkane proxy for the sedimentary input of submerged/floating freshwater aquatic macrophytes. Organic Geochemistry 31, 745–749.

He, Y., Zheng, Y., Pan, A., Zhao, C., Sun, Y., Song, M., Zheng, Z., Liu, Z., 2014. Biomarker-based reconstructions of Holocene lake-level changes at Lake Gahai on the northeastern Tibetan Plateau. The Holocene 24, 405–412.

Herzschuh, U., 2006. Palaeo-moisture evolution in monsoonal Central Asia during the last 50,000 years. Quaternary Science Reviews 25, 163–178.

Huang, X., Xue, J., Wang, X., Meyers, P.A., Huang, J., Xie, S., 2013a. Paleoclimate influence on early diagenesis of plant triterpenes in the Dajiuhu peatland, central China. Geochimica et Cosmochimica Acta 123, 106–119.

Huang, X., Meyers, P.A., Jia, C., Zheng, M., Xue, J., Wang, X., Xie, S., 2013b. Paleotemperature variability in central China during the last 13 ka recorded by a novel microbial lipid proxy in the Dajiuhu peat deposit. The Holocene 23, 1123–1129.

Jaatinen, K., Fritze, H., Laine, J., Laiho, R., 2007. Effects of short- and long-term water-level drawdown on the populations and activity of aerobic decomposers in a boreal peatland. Global Change Biology 13, 491–510.

Jones, M.C., Yu, Z., 2010. Rapid deglacial and early Holocene expansion of peatlands in Alaska. Proceedings of the National Academy of Sciences 107, 7347–7352.

Li, J., Zheng, Z., Huang, K., Yang, S., Chase, B., Valsecchi, V., Carré, M., Cheddadi, R., 2013. Vegetation changes during the past 40,000 years in Central China from a long fossil record. Quaternary International 310, 221–226.

Marzi, R., Torkelson, B.E., Olson, R.K., 1993. A revised carbon preference index. Organic Geochemistry 20, 1303–1306.

Mead, R., Xu, Y., Chong, J., Jaffé, R., 2005. Sediment and soil organic matter source assessment as revealed by the molecular distribution and carbon isotopic composition of *n*-alkanes. Organic Geochemistry 36, 363–370.

Nichols, J.E., Walcott, M., Bradley, R., Pilcher, J., Huang, Y., 2009. Quantitative assessment of precipitation seasonality and summer surface wetness using ombrotrophic sediments from an Arctic Norwegian peatland. Quaternary Research 72, 443–451.

Pancost, R.D., Baas, M., van Geel, B., Damste, J.S.S., 2002. Biomarkers as proxies for plant inputs to peats: an example from a sub-boreal ombrotrophic bog. Organic Geochemistry 33, 675–690.

Poynter, J., Eglinton, G., 1990. Molecular composition of three sediments from hole 717C: The Bengal Fan. In: Cochran, J.R., Stow, D.A.V. (Eds.), Proceedings of the Ocean Drilling Program. Scientific Results. College Station TX (Ocean Drilling Program) 116, pp. 155–161.

Reimer, P.J., Baillie, M.G., Bard, E., Bayliss, A., Beck, J.W., Blackwell, P.G., Ramsey, C.B., Buck, C.E., Burr, G.S., Edwards, R.L., et al., 2009. IntCal09 and Marine09 radiocarbon age calibration curves, 0–50,000 years cal BP. Radiocarbon 51, 1111–1150.

Sachse, D., Radke, J., Gleixner, G., 2006. δD values of individual n-alkanes from terrestrial plants along a climatic gradient—implications for the sedimentary biomarker record. Organic Geochemistry 37, 469–483.

Stuiver, M., Reimer, P.J., 1993. Extended ^{14}C data-base and revised Calib 3.0 ^{14}C age calibration program. Radiocarbon 35, 215–230.

Wang, Y., Cheng, H., Edwards, R.L., An, Z., Wu, J., Shen, C., Dorale, J.A., 2001. A high-resolution absolute-dated late pleistocene monsoon record from Hulu Cave, China. Science 294, 2345–2348.

Wang, Y., Cheng, H., Edwards, R.L., Kong, X., Shao, X., Chen, S., Wu, J., Jiang, X., Wang, X., An, Z., 2008. Millennial- and orbital-scale changes in the East Asian monsoon over the past 224,000 years. Nature 451, 1090–1093.

Xie, S., Evershed, R.P., Huang, X., Zhu, Z., Pancost, R.D., Meyers, P.A., Gong, L., Hu, C., Huang, J., Zhang, S., et al., 2013. Concordant monsoon-driven postglacial hydrological changes in peat and stalagmite records and their impacts on prehistoric cultures in central China. Geology 41, 827–830.

Zhao, C., Chang, Y., Chen, M., Liu, Z., 2013. Possible reverse trend in Asian summer monsoon strength during the late Holocene. Journal of Asian Earth Sciences 69, 102–112.

Zhao, Y., Yu, Z., Tang, Y., Li, H., Yang, B., Li, F., Zhao, W., Sun, J., Chen, J., Li, Q., Zhou, A., 2014. Peatland initiation and carbon accumulation in China over the last 50,000 years. Earth-Science Reviews 128, 139–146.

Zheng, Y., Zhou, W., Meyers, P.A., Xie, S., 2007. Lipid biomarkers in the Zoigê-Hongyuan peat deposit: indicators of Holocene climate changes in West China. Organic Geochemistry 38, 1927–1940.

Zhou, W., Xie, S., Meyers, P.A., Zheng, Y., 2005. Reconstruction of late glacial and Holocene climate evolution in southern China from geolipids and pollen in the Dingnan peat sequence. Organic Geochemistry 36, 1272–1284.

Zhou, W., Zheng, Y., Meyers, P.A., Jull, A.J.T., Xie, S., 2010. Postglacial climate-change record in biomarker lipid compositions of the Hani peat sequence, Northeastern China. Earth and Planetary Science Letters 294, 37–46.

Zhu, C., Ma, C., Yu, S.-Y., Tang, L., Zhang, W., Lu, X., 2010. A detailed pollen record of vegetation and climate changes in Central China during the past 16,000 years. Boreas 39, 69–76.

https://doi.org/10.1016/j.yqres.2015.06.004 Published online by Cambridge University Press